

elicit responses in c-MAF mutant carriers at high but not low frequencies (Fig. 3E). Tactile spatial acuity, that is, the ability to distinguish grids of different spacing, is thought to depend on hair follicle afferents/Meissner corpuscles/Merkel cell-neurite complexes (25, 28, 29) and was not significantly changed (fig. S6J). Thus, the R288P c-MAF mutation interferes with normal vibration detection in humans.

To understand the mechanism underlying mechanoreceptive deficits, we identified changes in gene expression in DRG neurons of c-Maf mutants. Ret and MafA expression was strongly reduced at birth as assessed by counting Ret⁺/NF200⁺ and MafA⁺ neurons (Fig. 4, A, B, and F) and modestly or not affected at E13.5 (fig. S7). Thus, c-Maf is required to maintain but not initiate Ret and MafA expression. We also analyzed DRGs of Ret mutant mice and found that c-Maf expression was unchanged (fig. S7). Thus, c-Maf acts upstream to maintain but not initiate Ret expression during RAM development.

We also examined the expression of receptors and ion channels characteristic of mechanoreceptors like TrkB, Ca_v3.2, and Piezo2, which were unchanged in c-Maf mutants (Fig. 4, C, D, and F, and fig. S7M). Further deregulated genes were identified by using microarray analysis and in situ hybridization. Among these were crystallins (Cryba2 and Crygs), known c-Maf targets encoding structural lens proteins (15). Crystallins also act as chaperones and can impinge on neural physiology. Further, genes encoding the potassium channels Kcng4, Kcnq4, Kcna1, and Kcnh5 were down-regulated in c-Maf mutants (Fig. 4, E and F, and table S1). Kcnq4 was recently found to fine-tune mechanoreceptor function (30). The Kcnq channel blocker linopirdine shortens interspike intervals of RAMs in control but not c-Maf mutants (Fig. 4, G and H), directly implicating Kcnq4 in one aspect of the functional changes that are observed in RAMs of c-Maf mutant mice.

Our analyses show that c-Maf directs mechanoreceptor development. c-Maf acts upstream of Ret, a receptor known to control RAM development, providing a mechanistic basis for this phenotype. c-Maf and MafA are similar in structure and might act redundantly. The fact that MafA expression is not maintained in c-Maf mutant mechanoreceptors can explain the salient function of c-Maf. c-Maf controls many parameters of RAM development, morphology, and function and modulates functional aspects of SAMs. Our analysis also reveals that the most strongly affected RAM subtype in the c-Maf mutant mice are Pacinian corpuscles that specialize in the detection of high-frequency vibration. Pacinian corpuscles and associated axons were largely absent, and residual corpuscles exhibited disrupted morphologies. Because the deformation of the lamellar end organ of Pacinian corpuscles initiates axonal firing (31), remaining corpuscles are expected to be functionally impaired. In line with this, humans carrying a dominant cataract-causing

c-MAF mutation displayed reduced acuity to high-frequency vibration. Other mechanisms like aberrant spinal processing of vibrotactile information might also contribute to this deficit in humans. We conclude that the transcription factor c-Maf directs RAM development and formation of RAM mechanoreceptive end organs.

References and Notes

1. Q. Ma, *Neuron* **64**, 773 (2009).
2. G. R. Lewin, Y. A. Barde, *Annu. Rev. Neurosci.* **19**, 289 (1996).
3. P. Delmas, J. Hao, L. Rodat-Despoix, *Nat. Rev. Neurosci.* **12**, 139 (2011).
4. M. Tsunozaki, D. M. Bautista, *Curr. Opin. Neurobiol.* **19**, 362 (2009).
5. F. Marmigère, P. Ernfors, *Nat. Rev. Neurosci.* **8**, 114 (2007).
6. Y. Liu, Q. Ma, *Curr. Opin. Neurobiol.* **21**, 52 (2011).
7. Q. Ma, C. Fode, F. Guillemot, D. J. Anderson, *Genes Dev.* **13**, 1717 (1999).
8. D. C. Molliver *et al.*, *Neuron* **19**, 849 (1997).
9. I. Kramer *et al.*, *Neuron* **49**, 379 (2006).
10. W. Luo, H. Enomoto, F. L. Rice, J. Milbrandt, D. D. Ginty, *Neuron* **64**, 841 (2009).
11. S. Bourane *et al.*, *Neuron* **64**, 857 (2009).
12. Y. Honma, M. Kawano, S. Kohsaka, M. Ogawa, *Development* **137**, 2319 (2010).
13. L. Lecoin *et al.*, *Dev. Neurobiol.* **70**, 485 (2010).
14. H. Motohashi, J. A. Shavit, K. Igarashi, M. Yamamoto, J. D. Engel, *Nucleic Acids Res.* **25**, 2953 (1997).
15. B. Z. Ring, S. P. Cordes, P. A. Overbeek, G. S. Barsh, *Development* **127**, 307 (2000).
16. R. V. Jamieson *et al.*, *Hum. Mol. Genet.* **11**, 33 (2002).
17. V. Vanita, D. Singh, P. N. Robinson, K. Sperling, J. R. Singh, *Am. J. Med. Genet. A.* **140**, 558 (2006).
18. L. Hansen *et al.*, *Invest. Ophthalmol. Vis. Sci.* **50**, 3291 (2009).
19. M. Z. Li *et al.*, *Dev. Biol.* **292**, 555 (2006).
20. M. Koltzenburg, C. L. Stucky, G. R. Lewin, *J. Neurophysiol.* **78**, 1841 (1997).
21. Type II lanceolate endings are TrkB^{high}, and TrkB^{high} neurons do not express c-Maf (<5%). TrkB^{high} neurons

- coexpress Ca_v3.2 and correspond thus to D-hairs (fig. S6A). Type III lanceolate endings are NF200⁺, and NF200⁻ neurons do not express c-Maf.
22. Heterogeneity of lanceolate endings was recently also noted by L. Li *et al.*, *Cell* **147**, 1615 (2011). They report that Aβ-, Aδ-, and C-low threshold mechanoreceptors terminate in lanceolate endings, and comparisons of marker expression indicate that these correspond to type I, II, and III endings, respectively.
 23. J. Zelená, *Prog. Brain Res.* **43**, 59 (1976).
 24. N. Rajaram, T. K. Kerppola, *Mol. Cell. Biol.* **24**, 5694 (2004).
 25. W. H. Talbot, I. Darian-Smith, H. H. Kornhuber, V. B. Mountcastle, *J. Neurophysiol.* **31**, 301 (1968).
 26. R. S. Johansson, A. B. Vallbo, *J. Physiol.* **297**, 405 (1979).
 27. K. O. Johnson, T. Yoshioka, F. Vega-Bermudez, *J. Clin. Neurophysiol.* **17**, 539 (2000).
 28. R. W. Van Boven, K. O. Johnson, *Neurology* **44**, 2361 (1994).
 29. S. J. Bensmaia, P. V. Denchev, J. F. Dammann 3rd, J. C. Craig, S. S. Hsiao, *J. Neurosci.* **28**, 776 (2008).
 30. M. Heidenreich *et al.*, *Nat. Neurosci.* **15**, 138 (2012).
 31. W. R. Loewenstein, M. Mendelson, *J. Physiol.* **177**, 377 (1965).

Acknowledgments: We are grateful to I. Schiffner, M. Terne, S. Buchert, C. Päseler, P. Stallerow, and the MDC transgenic and microarray units for technical support and animal husbandry and R. Schmidt-Ullrich, R. Hodge, A. Garratt, and W. Birchmeier (MDC, Berlin) for advice during analysis of hair types and critical reading of the manuscript. This work was funded by grants to C.B. and G.R.L. (SFB 665, NeuroCure). The authors declare no conflicts of interest.

Supporting Online Material

www.sciencemag.org/cgi/content/full/science.1214314/DC1
Materials and Methods
Figs. S1 to S7
Table S1
References (32–40)

21 September 2011; accepted 3 February 2012
Published online 16 February 2012;
10.1126/science.1214314

Niche and Neutral Effects of Acquired Immunity Permit Coexistence of Pneumococcal Serotypes

Sarah Cobey^{1*} and Marc Lipsitch^{1,2}

Over 90 capsular serotypes of *Streptococcus pneumoniae*, a common nasopharyngeal colonizer and major cause of pneumonia, bacteremia, and meningitis, are known. It is unclear why some serotypes can persist at all: They are more easily cleared from carriage and compete poorly in vivo. Serotype-specific immune responses, which could promote diversity in principle, are weak enough to allow repeated colonizations by the same type. We show that weak serotype-specific immunity and an acquired response not specific to the capsule can together reproduce observed diversity. Serotype-specific immunity stabilizes competition, and acquired immunity to noncapsular antigens reduces fitness differences. Our model can be used to explain the effects of pneumococcal vaccination and indicates general factors that regulate the diversity of pathogens.

The growing use of multivalent vaccines against antigenically variable pathogens creates a need to understand the individual-

and population-level forces that maintain the coexistence of pathogen strains so that the evolutionary effects of such vaccines can be anticipated. One

of the oldest ideas in ecology is that species are able to coexist by occupying unique niches (1). Stable coexistence involving a shared limiting resource can result when individuals compete more strongly with members of their own species than other species, creating a negative feedback loop that limits growth at high abundance (a stabilizing effect) (2). Among closely related pathogen strains, this kind of niche separation often arises through antigenic variation. By differing in their appearance to the immune system, competing strains effectively subdivide the host population, with each host a “habitat” more favorable to strains not yet encountered and for which strain-specific immunity is lacking. In this way, antigenic types to which few hosts are immune maintain a relative advantage. Niche partitioning through antigenic variation can explain the dynamics of protozoal (3), viral (4), and bacterial (5) pathogen populations and is a core assumption of theoretical models of strain competition (6).

Streptococcus pneumoniae, or pneumococcus, is a ubiquitous pathogen and a leading cause of pneumonia, meningitis, and bacteremia in children worldwide (7). The serotypes of pneumococcus are distinguished by their polysaccharide capsules. Licensed pneumococcal vaccines are serotype-specific and, despite overall benefits, have led to an increase in disease from nonvaccine serotypes. Thus, understanding the forces shaping pneumococcal serotype dynamics is important to interpret the effects of vaccine on disease and predict trends. Serotype-specific (henceforth, “anticapsular”) immunity might in principle provide a mechanism to maintain the diversity of pneumococcal serotypes. To permit coexistence, niche differences must be large enough to overcome differences in fitness that would otherwise lead to competitive exclusion (2). Many biological and epidemiological properties of pneumococcal strains, including properties that contribute directly to fitness, strongly correlate with the thickness of the capsule, which depends on the serotype. Serotypes with thicker capsules tend to have longer durations of nasopharyngeal carriage in young children (8), a competitive advantage in the nasopharynx (9), and a greater ability to escape neutrophil-mediated phagocytosis (10) in vitro, for example, compared with serotypes with thinner capsules. These traits also predict the prevalence of serotypes in carriage (9, 10), which is relatively consistent across human populations (text S1); Serotypes with thicker capsules are relatively more common. Studies of anticapsular immunity have shown, however, that the serotype-specific immunity elicited by natural exposure to pneumococci

is imperfect, frequently allowing repeated colonizations with the same serotype. Three separate studies have found evidence of strong immunity for one serotype (individuals who have carried type 14 are ~90% less likely to carry it again); however, they suggest that such immunity for all other serotypes, if it exists, is much less protective (e.g., point estimates of $\leq 50\%$ protection) (11–13). We sought to understand how such rel-

atively weak type-specific immune responses could support the coexistence of serotypes with substantial fitness differences.

To do so, we developed an individual-based model (text S2 to S5) constructed to avoid an intrinsic bias toward coexistence (14). We simulated the transmission dynamics of 25 serotypes that differed only in their intrinsic durations of carriage and their in vivo competitive abilities (15, 16).

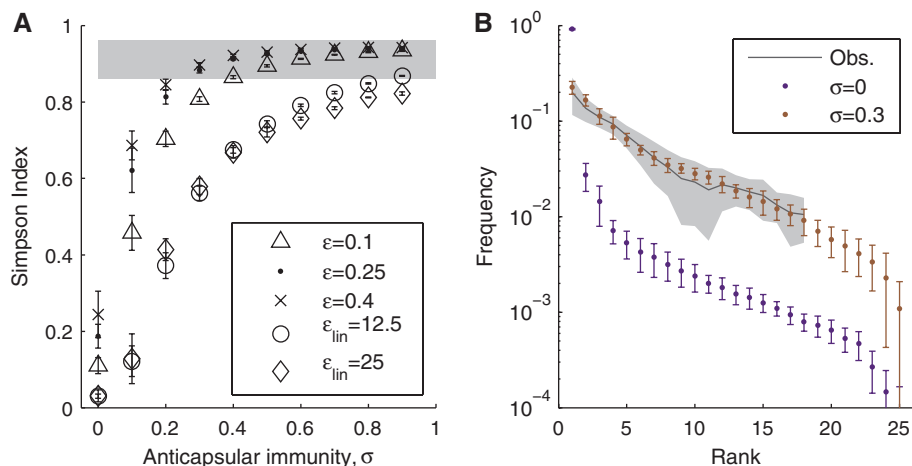
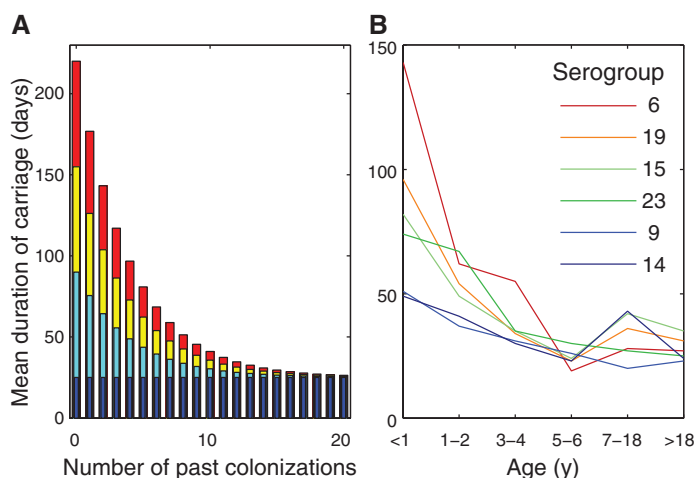


Fig. 1. Serotype diversity is sensitive to the form of acquisition of nonspecific immunity and the strength of anticapsular immunity. **(A)** Diversity, measured by the Simpson index, as a function of the strength of anticapsular immunity for different forms of acquired nonspecific immunity (durations that decay linearly to 0, $\epsilon_{lin} = 12.5$, and $\epsilon_{lin} = 25$; durations that decay exponentially to a nonzero value, $\epsilon = 0.10$, $\epsilon = 0.25$, and $\epsilon = 0.40$; text S4). The Simpson index equals the probability of randomly picking two serotypes from the population with replacement; it was calculated as $1 - D$, where $D = \sum p_i^2$, and p_i denotes the frequency of the i th species. Measures were obtained by averaging annual estimates of the Simpson index for each of the last 20 years of each simulation. The shaded area shows the range of diversity observed in carriage studies. **(B)** Observed (Obs.) rank-frequency distributions from carriage studies and the default model ($\epsilon = 0.25$) without ($\sigma = 0$) and with ($\sigma = 0.3$) anticapsular immunity. The gray line shows the mean distribution from carriage studies, and the shading indicates the SD (text S1). Error bars show SD based on 10 simulations.

Fig. 2. The rate of acquisition of nonspecific immunity was modeled as a linear or exponential function, with the latter supported by observations. **(A)** The duration of carriage of four serotypes modeled as an exponential function of the number of times a host previously cleared any serotype of pneumococcus ($\epsilon = 0.25$). The durations of the different serotypes are shown as superimposed bars, with the color indicating the serotype's fitness (red, most fit; blue, least fit). **(B)** Observed mean durations of carriage of different serogroups (serotypes or groups of antigenically related serotypes) as a function of host age from (8).



¹Center for Communicable Disease Dynamics and Department of Epidemiology, Harvard School of Public Health, 677 Huntington Avenue, Boston, MA 02115, USA. ²Department of Immunology and Infectious Diseases, Harvard School of Public Health, 677 Huntington Avenue, Boston, MA 02115, USA.

*To whom correspondence should be addressed. E-mail: scobey@hsph.harvard.edu

These two components of fitness were positively correlated: Serotypes with longer intrinsic durations of carriage were also better at excluding other serotypes in vivo (9). This competitive ability was modeled as a reduction in a host's susceptibility to a colonizing serotype, with the size of the reduction set by the fitness of any resident serotypes. Anticapsular immunity reduced a host's susceptibility to colonization by a fraction σ if the host had ever previously cleared that serotype (11). This fraction was the same for all serotypes but was varied across simulations. Because anticapsular immunity is thought to result from antibodies, once acquired, it was assumed to persist for the duration of a host's life. To facilitate comparisons of simulations involving different parameter values, we fitted transmission rates so that the total carriage prevalence of pneumococcus in children <5 years old was 40%. Simulations were run for 150 years, and serotype frequencies from the last 20 years were analyzed.

We first considered models with anticapsular immunity and acquired non-serotype-specific immunity (henceforth "nonspecific") that reduced each serotype's duration of carriage (17) by a fixed amount for every past exposure to any serotype (fig. S4). In these cases, the presence of anticapsular immunity, a stabilizing mechanism, promoted serotype diversity (Fig. 1A). However, anticapsular immunity alone was insufficient to overcome differences in serotypes' fitnesses: Even implausibly high levels of immunity (e.g.,

a 90% reduction in susceptibility from prior homologous carriage for each serotype) could not generate the high diversity observed in studies (text S6). Furthermore, high levels of anticapsular immunity in this scenario created an unrealistically low carriage prevalence and diversity in adults (text S6).

Epidemiologic studies of carriage duration (8) suggest that, as individuals acquire nonspecific immunity to pneumococcus, the duration of carriage declines for all serotypes, approaching a fixed value of several weeks in individuals with multiple exposures regardless of serotype (Fig. 2). This mechanism is thought to be largely driven by CD4⁺ T helper-17 cells (18, 19). Modeling this form of nonspecific immunity generated realistic patterns of diversity (Fig. 1 and text S6). A consequence of this nonlinear decline in duration is that, in highly exposed individuals, the fitness advantage of the "best" serotypes is reduced because their durations fall disproportionately (9). Acquired nonspecific immunity thus reduces fitness variation between serotypes, and this reduction is most pronounced in older individuals. This phenomenon might explain the higher diversity of serotypes (in both carriage and invasive disease) in older children and adults (20, 21). Some anticapsular immunity remains necessary in this scenario, underscoring the joint contribution of niche (stabilizing) and neutral (equalizing) mechanisms to coexistence (Fig. 1B) (2). In general, the simulated serotype distributions match observed distributions when

anticapsular immunity confers a 30 to 60% reduction in susceptibility to future colonizations with that type (Fig. 1B and fig. S9). This estimate is consistent with the finding that the confidence intervals of serotype-specific reductions in susceptibility from prior homologous carriage overlap in the range of 34 to 36% (11).

Models with intermediate levels of anticapsular immunity and a nonlinear reduction in the duration of carriage with exposure reproduced other key aspects of pneumococcal dynamics. These models produced relatively consistent rankings of serotype frequencies across populations, a realistic reduction in the duration of carriage with age, higher pneumococcal diversity in adults than in children, and realistic rates of co-colonization (Table 1). Large, multiannual fluctuations in the abundance of rarer serotypes were a common feature in models with anticapsular immunity, and similar fluctuations have been observed in time series of disease isolates (text S6.6) (22).

The major results were robust to the size of the host population, the rate of immigration, and the rate of acquiring nonspecific immunity, and they were modestly affected by host population structure and the total prevalence of pneumococcus (text S6.7 to S6.11). Quantitative validation of our model is limited, however, by the uncertainty in the actual intrinsic durations and transmissibilities of serotypes in nature. Our model assumed that serotypes were

Table 1. Assumptions and constraints of the model and patterns reproduced by the calibrated model. The first section lists the major assumptions of the models and the empirical support for these assumptions. The second section lists the criteria by which the different models of immunity were judged. The

third section lists additional patterns reproduced by the calibrated model ($\sigma = 0.3$, $\epsilon = 0.25$). For each pattern, the supporting figure(s) and the supplementary text sections in which the competing immune models are judged are also listed. Dash entries indicate not applicable.

	Figure	Description/reference
<i>Epidemiologic observations used to define model assumptions</i>		
Weak to nonexistent anticapsular immunity	–	(11–13), text S2
Reduction in the duration of carriage from nonspecific immunity	1	(17–19, 22), text S2 and S4.1
In vivo competition strength correlating with serotype fitness (duration of carriage)	–	(9, 15), text S2
<i>Model outputs used to calibrate parameter values and functional forms</i>		
Total carriage prevalence in children <5 years old	–	Table S1
Diversity (Simpson index)	1A	Main text
Rank-frequency distribution	1B, S9	Text S1 and S6.2
<i>Observed patterns reproduced by the calibrated model</i>		
Stability of rank order	S8, S10	Text S1 and S6.2
Decline in carriage duration with age	S11	text S6.3
Increase in serotype diversity with age	S12	Text S1 and S6.4
Frequency of co-colonizations	S13	Text S6.5
Epidemics of rarer serotypes	S14, S15	Text S6.6
Serotype replacement after vaccination	3, A and B	Main text
Brief increase in diversity after vaccination	3C	Main text

equally infectious per day (in the absence of evidence to the contrary) and had evenly distributed intrinsic durations of carriage. Consistent with theory (2), patterns of diversity were sensitive to the density of serotypes within this range (fig. S16). For example, when we simulated 15 serotypes instead of 25 within the same range, more anticapsular immunity (higher σ) was required to overcome the larger differences in fitness between serotypes. With 35 serotypes, slightly less anticapsular immunity was needed. Our model used a relatively dense packing of fitnesses (text S4.1), implying that the conditions we identify that promote diversity are conservative requirements.

The dynamics of serotypes competing through naturally acquired immunity shed light on serotype replacement after vaccination. Unlike natural colonization, the pneumococcal conjugate vaccine induces anticapsular immunity that is strongly protective against future carriage (23). We expanded our model to include vaccination, assuming that vaccine-induced immunity, like naturally induced anticapsular immunity, permanently reduced susceptibility to future colonizations with specific serotypes. The strengths of natural and vaccine-acquired immunity were varied across simulations. Simulating vaccination with realistic parameters reproduced the observed

rapid and sustained replacement of serotypes targeted by the vaccine (24) when the anticapsular immunity induced by the vaccine was stronger than the naturally occurring form (Fig. 3, A and B). In many scenarios, serotype diversity briefly increased in the few years after vaccination, a trend observed in human populations (Fig. 3C and text S7) (24, 25). In addition, introduction of the simulated vaccine caused the prevalence of total carriage to fluctuate before approaching a new equilibrium (Fig. 3D). In human populations, changes in overall carriage postvaccination have ranged from small increases to large decreases (text S7.2). Whether the simulated serotype diversity or total carriage prevalence ultimately returned to prevaccine levels depended on the ranks of the targeted serotypes (text S7.1). All nonvaccine serotypes increased in frequency after vaccine introduction in approximate proportion to their prevaccine frequencies (Fig. 3E). The precise effects of vaccination on carriage and invasive disease probably depend on the extent of natural versus vaccine-induced cross-immunity between potentially cross-reacting serotypes: Certain serogroups (6, 19, and 23) contain several antigenically similar serotypes, of which only one was in the heptavalent conjugate vaccine (26) (text S7.1). Effects might also depend on the vaccination schedule and rate of introduction and

the efficacy of the vaccine with respect to each serotype.

A theoretically interesting prediction of the model is that sustained reductions in anticapsular and/or nonspecific immunity after vaccination can allow previously excluded serotypes to reinvade successfully if introduced through immigration. If vaccine-induced, serotype-specific immunity to carriage is weaker than that obtained through natural exposure, targeted serotypes can resurge after several years to decades (Fig. 3F). This transient period of low prevalence after vaccination is similar to the “honeymoon period” after a vaccine introduction at a coverage just below what is required to eliminate transmission through herd immunity (27). Instead of arising from unvaccinated individuals, the resurgence here comes from incomplete immunity, particularly a reduction in anticapsular immunity. Even when vaccine-induced immunity is stronger than natural immunity, if total carriage drops precipitously from vaccination, the resulting decline in nonspecific immunity can also permit the return of previously eradicated serotypes (fig. S18).

Previous efforts to model carriage of nasopharyngeal colonizing bacteria have focused on vaccine effects and have assumed, rather than tried to explain, coexistence of serotypes (28–30).

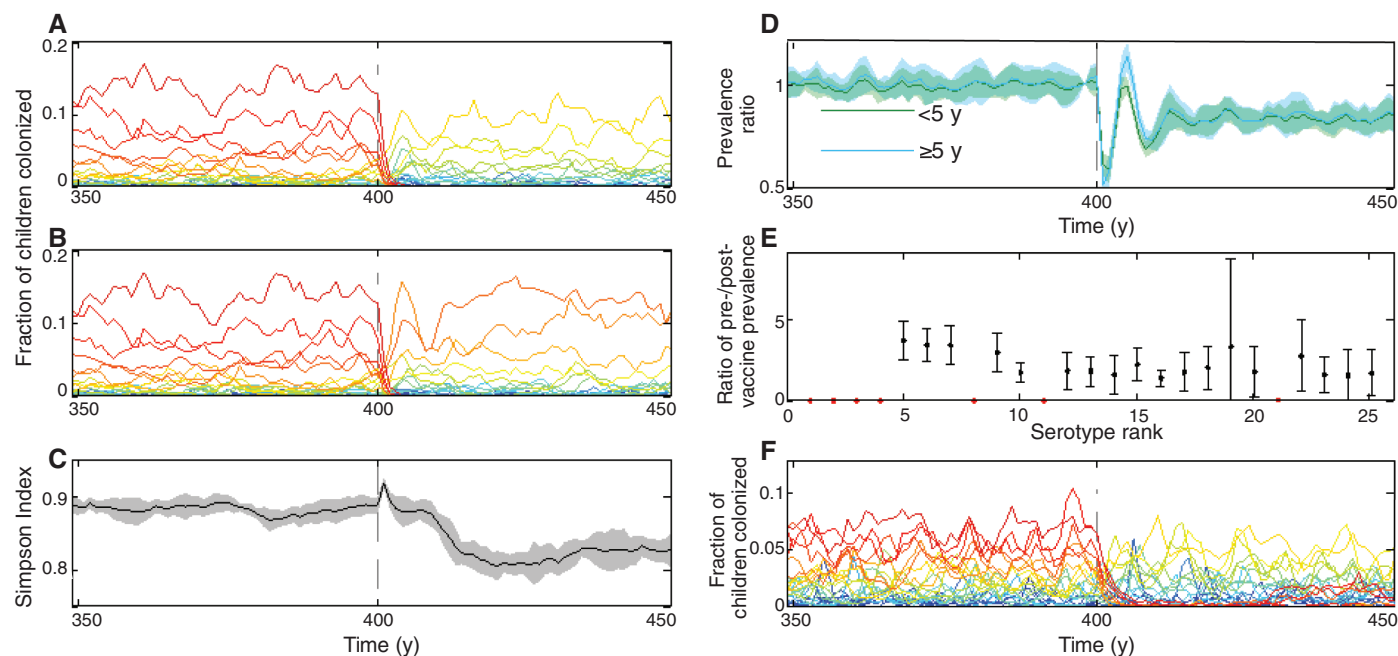


Fig. 3. Vaccination causes at least short-term serotype replacement and can lower total carriage. (A and B) Sample dynamics involving vaccination assuming $\sigma = 0.3$. The prevalences (in children <5 years old) of individual serotypes, colored by their intrinsic fitness as in Fig. 2, are shown. The vaccine was given to all children 6 months old starting in year 400 (dashed line) and had a 60% efficacy against targeted serotypes: (A) Vaccination targeting the seven most intrinsically fit serotypes (ranks 1 to 7). (B) Vaccination targeting serotypes with ranks analogous to those included in the heptavalent pneumococcal conjugate vaccine (ranks 1 to 4, 8, 11, and

21; text S7.1). (C) Simpson index in children <5 years from the scenario in (B). (D) Total carriage prevalence (as a ratio of each year's prevalence to the prevalence in year 399) over time in children <5 years and in individuals ≥ 5 years from the scenario in (B). (E) The ratio of each serotype's postvaccine prevalence (its mean prevalence in years 410 to 419) to its prevaccine prevalence (years 300 to 399) from the scenario in (B). Targeted serotypes are in red. In (C) to (E), shading or error bars show SD based on 10 simulations. (F) As in (A), vaccination targeting the seven fittest serotypes but with natural immunity ($\sigma = 0.7$) stronger than vaccine-induced immunity.

This study has shown that the diversity of a pathogen can be maintained simply by the interaction of acquired specific and nonspecific immunity, despite fitness differences between serotypes. The sensitivity of the results to the distribution of simulated serotypes' growth rates raises the intriguing question of what upper limits exist for the number of pathogen strains that can coexist stably in a host population and how this depends on the relation between their antigenicity and intrinsic fitness (31). More broadly, this study supports a growing perspective in ecology that recognizes the joint role of niche and neutral dynamics in shaping diversity (2, 32). As antigen-specific vaccines are introduced against pathogens such as human papillomavirus, meningococcus, malaria, and other polymorphic infections, these findings suggest that attention to the details of immune responses may be required to explain prevaccine patterns and make predictions about the effects of vaccines on pathogen populations.

References and Notes

- G. E. Hutchinson, *Quant. Bio.* **22**, 415 (1957).
- P. Chesson, *Annu. Rev. Ecol. Syst.* **31**, 343 (2000).
- C. O. Buckee, P. C. Bull, S. Gupta, *Proc. Biol. Sci.* **276**, 477 (2009).
- K. Koelle, S. Cobey, B. Grenfell, M. Pascual, *Science* **314**, 1898 (2006).
- C. O. Buckee, S. Gupta, P. Kriz, M. C. Maiden, K. A. Jolley, *Proc. Biol. Sci.* **277**, 1635 (2010).
- S. Gupta, N. M. Ferguson, R. M. Anderson, *Science* **280**, 912 (1998).
- K. L. O'Brien *et al.*, *Lancet* **374**, 893 (2009).
- L. Högberg *et al.*, *J. Clin. Microbiol.* **45**, 948 (2007).
- M. Lipsitch *et al.*, *Epidemiology* 10.1097/EDE.0b013e31824f2f32 (2012).
- D. M. Weinberger *et al.*, *PLoS Pathog.* **5**, e1000476 (2009).
- D. M. Weinberger *et al.*, *J. Infect. Dis.* **197**, 1511 (2008).
- P. C. Hill *et al.*, *Clin. Infect. Dis.* **46**, 807 (2008).
- D. Goldblatt *et al.*, *J. Infect. Dis.* **192**, 387 (2005).
- M. Lipsitch, C. Colijn, T. Cohen, W. P. Hanage, C. Fraser, *Epidemics* **1**, 2 (2009).
- M. Lipsitch *et al.*, *Vaccine* **18**, 2895 (2000).
- E. S. Lysenko, R. S. Lijek, S. P. Brown, J. N. Weiser, *Curr. Biol.* **20**, 1222 (2010).
- B. M. Gray, G. M. Converse 3rd, H. C. Dillon Jr., *J. Infect. Dis.* **142**, 923 (1980).
- Y. J. Lu *et al.*, *PLoS Pathog.* **4**, e1000159 (2008).
- R. Malley *et al.*, *Proc. Natl. Acad. Sci. U.S.A.* **102**, 4848 (2005).
- O. Abdullahi, J. Nyiro, P. Lewa, M. Slack, J. A. Scott, *Pediatr. Infect. Dis. J.* **27**, 59 (2008).
- W. P. Hausdorff, J. Bryant, C. Kloek, P. R. Paradiso, G. R. Siber, *Clin. Infect. Dis.* **30**, 122 (2000).
- Z. B. Harboe *et al.*, *Clin. Infect. Dis.* **50**, 329 (2010).
- H. Rinta-Kokko, R. Dagan, N. Givon-Lavi, K. Auranen, *Vaccine* **27**, 3831 (2009).
- W. P. Hanage *et al.*, *Epidemics* **2**, 80 (2010).
- S. Flasche *et al.*, *PLoS Med.* **8**, e1001017 (2011).
- X. Yu *et al.*, *J. Infect. Dis.* **180**, 1569 (1999).
- A. R. McLean, *Br. Med. Bull.* **54**, 545 (1998).
- M. Lipsitch, *Proc. Natl. Acad. Sci. U.S.A.* **94**, 6571 (1997).
- A. Melegaro, Y. Choi, R. Pebody, N. Gay, *Am. J. Epidemiol.* **166**, 228 (2007).
- C. L. Trotter, N. J. Gay, W. J. Edmunds, *Am. J. Epidemiol.* **162**, 89 (2005).
- R. MacArthur, R. Levins, *Am. Nat.* **101**, 377 (1967).
- P. B. Adler, J. Hillerislambers, J. M. Levine, *Ecol. Lett.* **10**, 95 (2007).

Acknowledgments: We thank O. Abdullahi and A. Scott for sharing their data on the duration of carriage; E. Lee for help reviewing carriage studies; C. Laine for sharing an unpublished earlier review of such studies; and C. Buckee, W. Hanage, B. Levin, R. Malley, V. Pitzer, D. Weinberger, and J. Zelnor for helpful comments. Computations were run on the Odyssey cluster supported by the FAS Science Division Research Computing Group at Harvard University. E-mail scobey@hsph.harvard.edu for the location of the code repository. The project was supported by awards 5R01AI048935 from the National Institute of Allergy and Infectious Diseases (NIAID) and 1F32GM097997 and U54GM088558 from the National Institute of General Medical Sciences (NIGMS). The content is solely the responsibility of the authors and does not necessarily represent the views of the NIGMS, NIAID, or the NIH. M.L. has received consulting fees or honoraria from Pfizer, Novartis, AIR Worldwide, and the Avian/Pandemic Flu Registry (Outcome Sciences), supported by Roche.

Supporting Online Material

www.sciencemag.org/cgi/content/full/science.1215947/DC1
Materials and Methods
Figs. S1 to S18
Tables S1 to S3
References (33–76)

28 October 2011; accepted 16 February 2012
Published online 1 March 2012;
10.1126/science.1215947



Niche and Neutral Effects of Acquired Immunity Permit Coexistence of Pneumococcal Serotypes

Sarah Cobey and Marc Lipsitch

Science **335**, 1376 (2012);

DOI: 10.1126/science.1215947

This copy is for your personal, non-commercial use only.

If you wish to distribute this article to others, you can order high-quality copies for your colleagues, clients, or customers by [clicking here](#).

Permission to republish or repurpose articles or portions of articles can be obtained by following the guidelines [here](#).

The following resources related to this article are available online at www.sciencemag.org (this information is current as of November 30, 2015):

Updated information and services, including high-resolution figures, can be found in the online version of this article at:

<http://www.sciencemag.org/content/335/6074/1376.full.html>

Supporting Online Material can be found at:

<http://www.sciencemag.org/content/suppl/2012/03/01/science.1215947.DC1.html>

This article **cites 72 articles**, 33 of which can be accessed free:

<http://www.sciencemag.org/content/335/6074/1376.full.html#ref-list-1>

This article has been **cited by** 14 articles hosted by HighWire Press; see:

<http://www.sciencemag.org/content/335/6074/1376.full.html#related-urls>

This article appears in the following **subject collections**:

Microbiology

<http://www.sciencemag.org/cgi/collection/microbio>